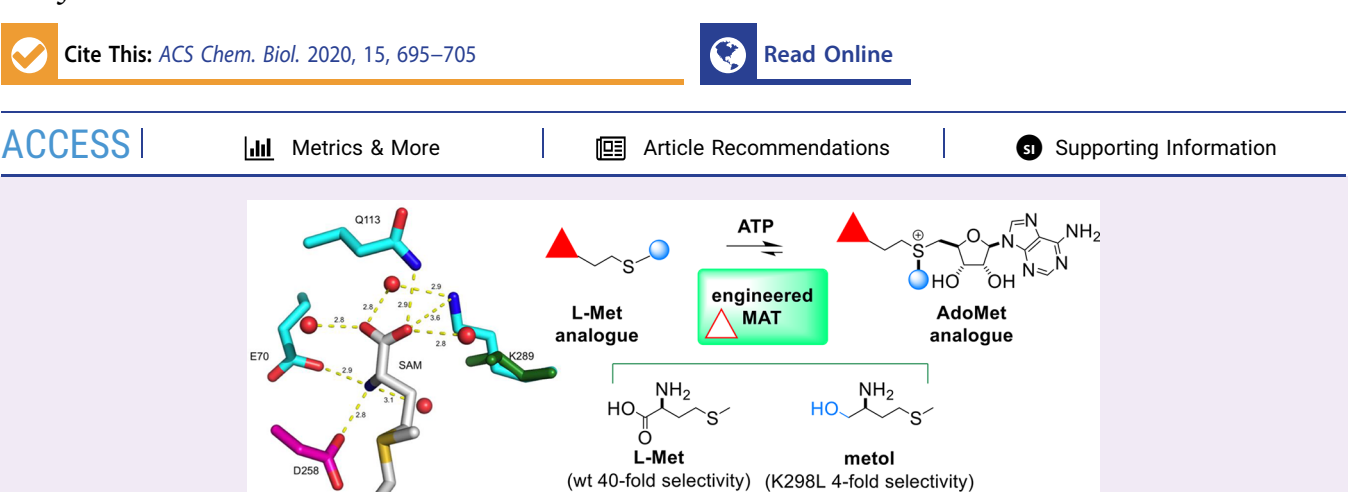


pubs.acs.org/acschemicalbiology Articles

Methionine Adenosyltransferase Engineering to Enable Bioorthogonal Platforms for AdoMet-Utilizing Enzymes

Tyler D. Huber, Jonathan A. Clinger, Yang Liu, Weijun Xu, Mitchell D. Miller, George N. Phillips, Jr.,* and Jon S. Thorson*



ABSTRACT: The structural conservation among methyltransferases (MTs) and MT functional redundancy is a major challenge to the cellular study of individual MTs. As a first step toward the development of an alternative biorthogonal platform for MTs and other AdoMet-utilizing enzymes, we describe the evaluation of 38 human methionine adenosyltransferase II-α (hMAT2A) mutants in combination with 14 non-native methionine analogues to identify suitable bioorthogonal mutant/analogue pairings. Enabled by the development and implementation of a hMAT2A high-throughput (HT) assay, this study revealed hMAT2A K289L to afford a 160-fold inversion of the hMAT2A selectivity index for a non-native methionine analogue over the native substrate L-Met. Structure elucidation of K289L revealed the mutant to be folded normally with minor observed repacking within the modified substrate pocket. This study highlights the first example of exchanging L-Met terminal carboxylate/amine recognition elements within the hMAT2A active-site to enable non-native bioorthgonal substrate utilization. Additionally, several hMAT2A mutants and L-Met substrate analogues produced AdoMet analogue products with increased stability. As many AdoMet-producing (e.g., hMAT2A) and AdoMet-utilizing (e.g., MTs) enzymes adopt similar active-site strategies for substrate recognition, the proof of concept first generation hMAT2A engineering highlighted herein is expected to translate to a range of AdoMet-utilizing target enzymes.

ethyltransferase (MT)-catalyzed transfer of the activated S-adenosyl-L-methionine (AdoMet) contributes to the functional modulation of biomolecules ranging from small metabolites $^{1-5}$ to macromolecules. $^{5,6,7-15}$ Alterations in methylation-dependent processes are associated with cancer, 16 neurodegenerative/neuropsychiatric disorders, ^{17–19} inflammation, ^{20,21} metabolic disorders, ²² fundamental development/ regenerative medicine, ^{23,24} susceptibility to disease/adverse drug response, ^{25,26} and drug resistance. ^{13–15,27,28} Yet, the structural conservation among MTs and a large array of discrete and redundant MTs in any given cell presents major challenges to the direct study of individual MTs in situ. 14,29-33 On the basis of proof of concept studies that revealed MTs to utilize non-native AdoMet analogues to afford differential alkylation,³⁴⁻³⁶ similar approaches have leveraged MT promiscuity and differentially-S-alkylated AdoMet analogues for MT-catalyzed alkylation of DNA/RNA, 34,37-50 proteins, 30,51-64 and bioactive secondary metabolites. 31,61,65-70 This conceptual advance, and the corresponding chemical biology reagents developed, enabled more recent efforts to

develop bioorthogonal allele-specific chemical genetics strategies (also referred to as "bump-and-hole")^{71–79} for intracellular metabolic profiling of individual MTs.^{29,59,60} Such bioorthogonal approaches employ an engineered target MT with complementary non-native AdoMet cosubstrates and seek to achieve orthogonal biochemically competent catalysis that uniquely distinguishes (via delivery of chemoselective tags) the intracellular function of the target MT. Current efforts, which rely on varying the S-alkyl substituent as the bioorthogonal element, remain hampered by selectivity as most, if not all, of the non-native S-alkyl AdoMet analogues employed to date for bioorthogonal applications remain substrates for wild-type

Received: November 22, 2019 Accepted: February 24, 2020 Published: February 24, 2020



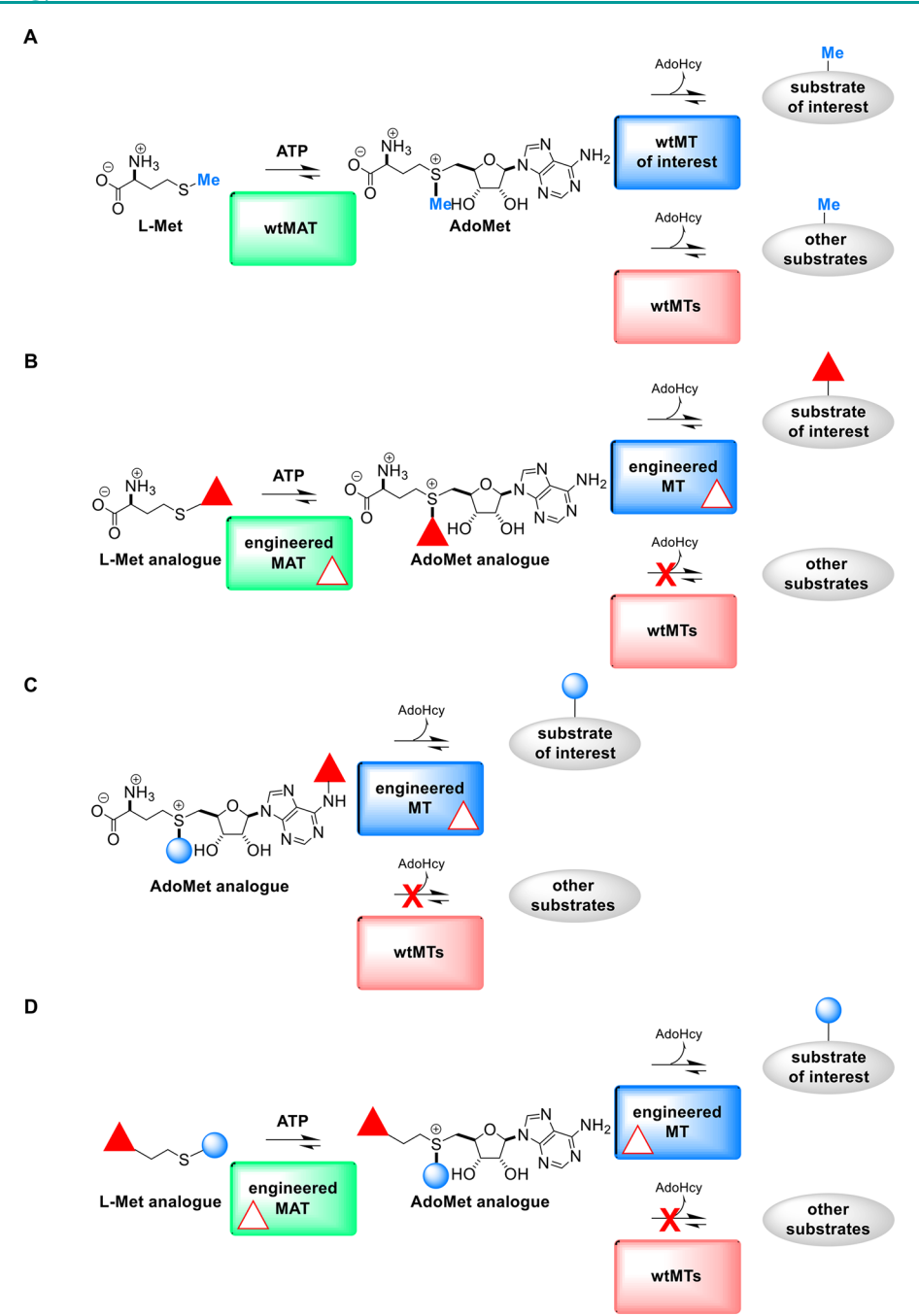


Figure 1. Complementary approaches to AdoMet-producing/utilizing enzyme bioorthogonal platform development. (A) Native function of representative AdoMet-producing/utilizing enzymes. In this context, AdoMet serves as the central substrate for all AdoMet-utilizing enzymes (including, but not limited to, methyltransferases). (B) S-alkyl-based bioorthogonal approach where steric bulk of the substrate S-alkyl substituent (represented by a triangle), paired with the appropriate AdoMet-producing/utilizing enzyme mutants, serves as the bioorthogonal differentiator. (C) Nucleoside-based bioorthogonal approach where a sterically modified nucleoside (structural modification represented by a triangle), paired with the appropriate AdoMet-producing/utilizing enzyme mutants, serves as the bioorthogonal differentiator. (D) Carboxylate/amino-terminibased bioorthogonal approach where alternative substrate-termini binding modalities (structural modification represented by a triangle), paired with the appropriate AdoMet-producing/utilizing enzyme mutants, serve as the bioorthogonal differentiator. MAT, methionine adenosyltransferase; MT, methyltransferase; AdoHcy, S-adenosyl-L-homocysteine; AdoMet, S-adenosylmethionine (SAM).

MTs. ^{59,60,63,80,81} While MTs are also known to accommodate modifications to the AdoMet adenine ⁸² or terminal carboxylate, ⁸³ attempts to exploit adenine and/or carboxylate alteration for bioorthogonal reagent development have been hampered, in part, by synthetic/commercial access to corresponding AdoMet analogues.

As a first step toward alternative formats for bioorthogonal design (Figure 1), herein we describe the evaluation of a range

of putative bioorthogonal human methionine adenosyltransferase II- α (hMAT2A) mutations and methionine analogues, the emphasis of which focused on modulation of hMAT2A binding interactions with the L-methionine (L-Met) terminal carboxylate and α -amine. Specifically, we describe the evaluation of 38 unique hMAT2A mutants (deriving from site-directed mutagenesis at four different active-site residues) with 14 non-native methionine analogues modified at the

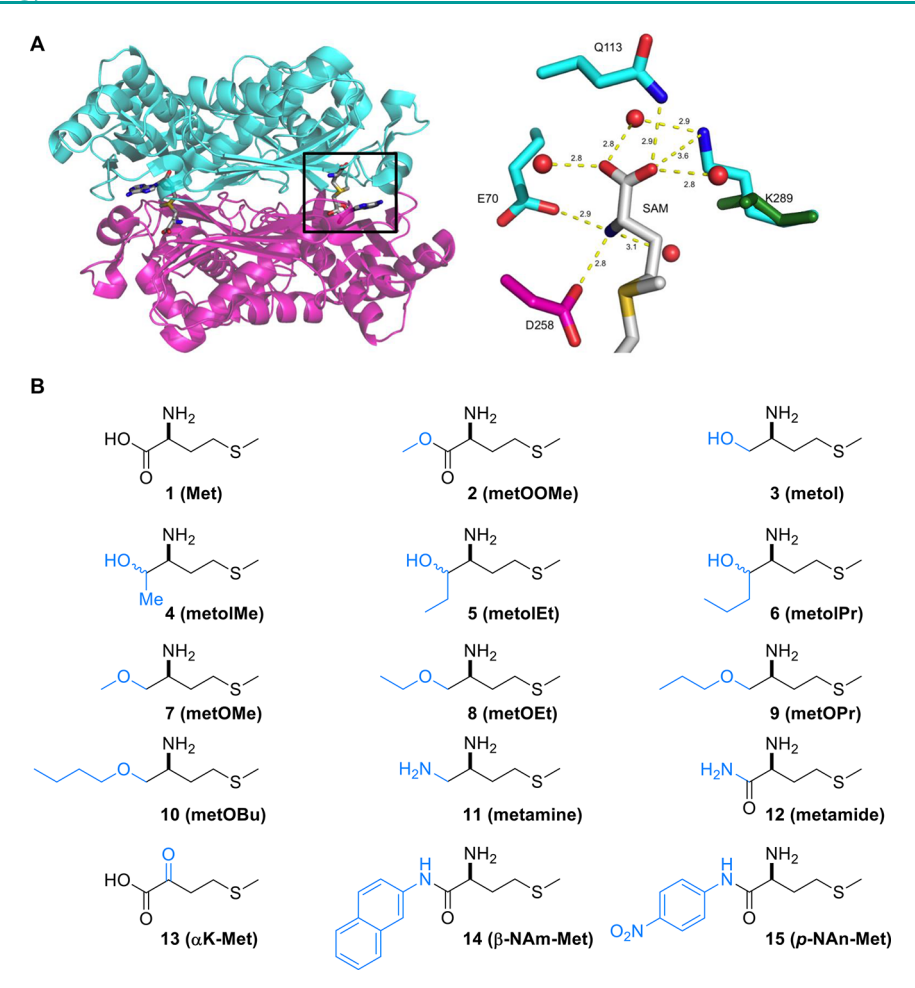


Figure 2. (A) Active-site of ligand-bound hMAT2A (PDB: 2P02) with key conserved active-site residues targeted for mutagenesis highlighted. Distances between targeted active-site amino acid side chains and the AdoMet (white) carboxylate oxygen or ammonium nitrogen are highlighted in yellow. The location of the isobutyl side chain of the K289L mutant as determined by X-ray crystallography in the current study is highlighted in green (PDB: 6P9V). (B) L-Met substrate surrogates used in the current study. Met, L-methionine; metOOMe, L-methionine methyl ester; metol, (S)-(-)-methioninol; metolMe, (3S)-3-amino-5-(methylthio)pentan-2-ol; metOMe, (S)-1-methoxy-4-(methylthio)butan-2-amine; metOEt, (S)-1-ethoxy-4-(methylthio)butan-2-amine; metOPr, (S)-4-(methylthio)-1-propoxybutan-2-amine; metOBu, (S)-1-butoxy-4-(methylthio)butan-2-amine; metamine, (S)-4-(methylthio)butane-1,2-diamine; metamide, (S)-2-amino-4-(methylthio)butanamide; αK-Met, α-keto-γ-(methylthio)-butyric acid; β-NAm-Met, L-methionine-β-naphthylamide; p-NAn-Met, L-methionine p-nitroanilide.

terminal carboxylate and/or α -amine. Enabled by the development and implementation of a hMAT2A high-throughput (HT) assay, this assessment revealed hMAT2A K289L to display a 160-fold inversion of the hMAT2A selectivity index for the non-native methionine analog S-(-)-methioninol (metol) over L-Met. Subsequent structural studies of K289L were consistent with design principles, and notably, the product of the K289L/metol reaction (AdoMetol) was also found to be resistant to the classical AdoMet intramolecular cyclization degradation pathway.^{83–87} This study also revealed that mutation of hMAT2A D258 may induce putative ATPase function. This work provides additional insights regarding hMAT2A substrate recognition and sets the stage for similar conceptual engineering of a paired AdoMet-utilizing enzyme (e.g., an engineered complementary MT) to provide the basis for a general bioorthogonal platform.

RESULTS AND DISCUSSION

Bioorthogonal Design for Mutagenesis and Methionine Analogue Synthesis. Our overarching goal was to develop hMAT2A mutants with demonstrated selectivity for

non-native methionine analogues over the native hMAT2A substrate L-Met. To achieve this goal, disruption of four key hMAT2A active-site side chain interactions with L-Met terminal carboxylate and α -amine were targeted (E70, Q113, D258, and K289; Figure 2A). Potential anticipated alternative non-native substrate binding interactions included (Figure 2A and B): modifications of electrostatic complementarity [e.g., pairing mutants K289D/E or Q113D/E with metamine (11) or metamide (12) or E70R/H/K or D258H/N mutants with methionine analogue α K-Met (13)]; potential alternative van der Waal's interactions [e.g., pairing mutants Q113A/V/I/L/ M/W or K289A/V/I/L/M/F/Y with methionine analogues metOOMe (2), metolMe (4), metolEt (5), metolPr (6), or methionine ethers (7-10)]; or varied hydrogen-bonding interactions [e.g., pairing mutants Q113T or K289C/S/T with metol (3)]. Commercially available L-methionine- β naphthylamide (14) and L-methionine p-nitroanilide (15) were also included as additional possible substrate surrogates. This conceptual design was inspired, in part, by our recent discovery that L-Met carboxylate isosteres were hMAT2A substrates of hMAT2A, where the corresponding AdoMet analogues were also both stable to rapid degradative intra-

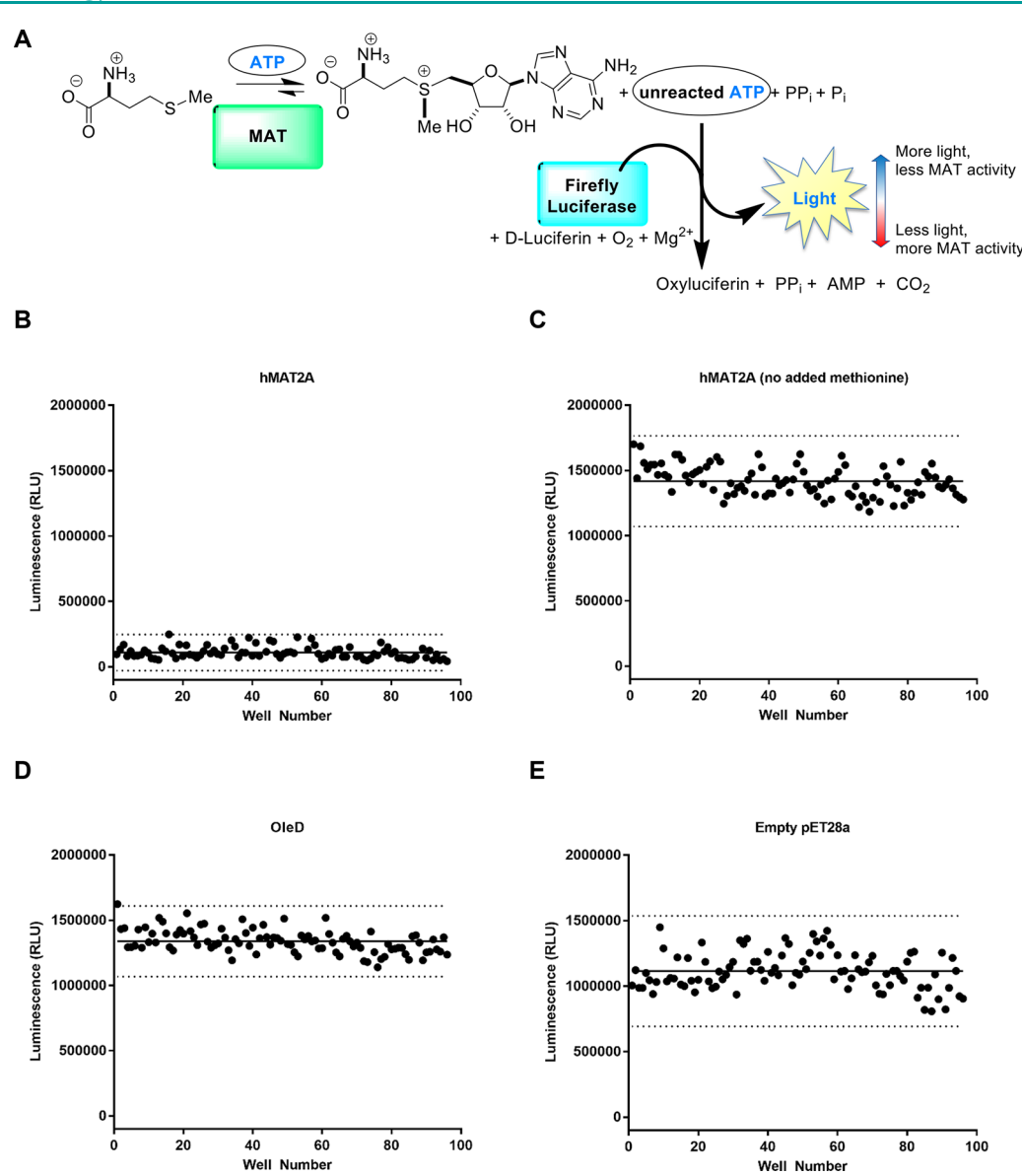


Figure 3. Plate-based hMAT2A assay development and validation. (A) hMAT2A reaction scheme and bioactivity detection strategy. (B) Wild-type hMAT2A *E. coli* extract (5μ L) with L-Met (10 mM) and ATP (1.5 mM), positive control. (C) Wild-type hMAT2A *E. coli* extract (5μ L) with ATP (1.5 mM) but lacking L-Met, negative control, Z' value of 0.63. (D) Glucosyltransferase OleD *E. coli* extract (nonreactive protein, 0.005 mL) with L-Met (10 mM) and ATP (1.5 mM), negative control, Z' value of 0.67. (E) Empty pET-28a *E. coli* extract (0.005 mL) with L-Met (10 mM) and ATP (1.5 mM), negative control, Z' value of 0.44. For panels B–E, each point represents determined raw luminescence units (RLU) from a single reaction/well. Comparison of RLU of positive and negative controls was used to calculate Z' values. Solid lines indicate population mean; dotted lines indicate population mean ± 3 standard deviations.

molecular cyclization and functional as MT substrates.⁸³ Substrate surrogates **4–6** were synthesized from commecially available *N*-Fmoc-L-methionine in four steps with overall yields ranging from 15–18%, while analogues **7–10** were constructed from commercially available *N*-Boc-L-methioninol in two steps with overall yields ranging from 49 to 81% (see Supporting Information for details regarding the syntheses and/or sourcing of all other L-Met surrogates employed).

Assay Development and Validation. A standard luciferase-based assay for [ATP] (Promega Corporation, Kinase-Glo Max) was used as a basis for 384-well plate-based assay development and the subsequent primary screen. While the reported intracellular concentration of ATP in *E. coli* $(1.54 \text{ mM})^{88}$ surpasses the linear range of the assay (linear up to 500 μ M ATP), ATP quickly depletes in cellular extracts.

Endogenous [ATP] added to the assay and post-lysis assay incubation time were optimized to maximize change in luminescence between the positive and negative controls to obtain a Z' value >0.5 (Figure 3). Optimized reaction conditions contained 10 mM L-Met and 1.5 mM ATP in 25 mM Tris·HCl (pH 8.0) containing 10 mM MgCl₂ and 50 mM KCl incubated at 37 °C for 1 h prior to incubation at ambient temperature for 20 min. Negative controls for assay validation and Z' value determination included pET28a-E. coli BL21 extract (empty vector control), pET28a/wtOleD-E. coli BL21 extract (nonspecific protein overproduction strain; macrolide glucosyltransferase OleD), 90,91 and assays with pET28a/hMAT2A-E. coli BL21 extract lacking L-Met. On the basis of comparison to the positive control (pET28a/hMAT2A-E. coli BL21), three separate Z' values were calculated (pET-28a

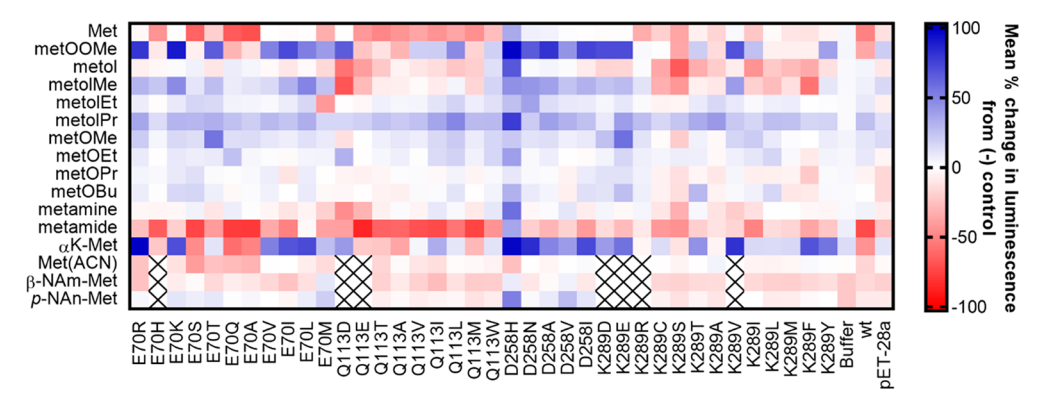


Figure 4. Combinatorial plate-based screen of targeted hMAT2A mutants with L-Met analogues highlighted in Figure 2. The heat map compares the relative activity of hMAT2A mutant (y-axis) and L-Met analogue (x-axis) pairings. The color of each square is dependent on the percent change in mean relative luminescence units (RLU) under experimental conditions from the mean RLU of the negative control (no added methionine or analogue thereof in the reaction mixture) for that mutant. Red corresponds to lower observed luminescence (i.e., lower [ATP]) as an indirect measure of turnover; blue indicates higher observed luminescence (i.e., higher [ATP]) as an indirect measure of lack of turnover; X, not tested. Standard assay conditions: 10 mM L-Met analogue, 1.5 mM ATP, 37 °C, 60 min.

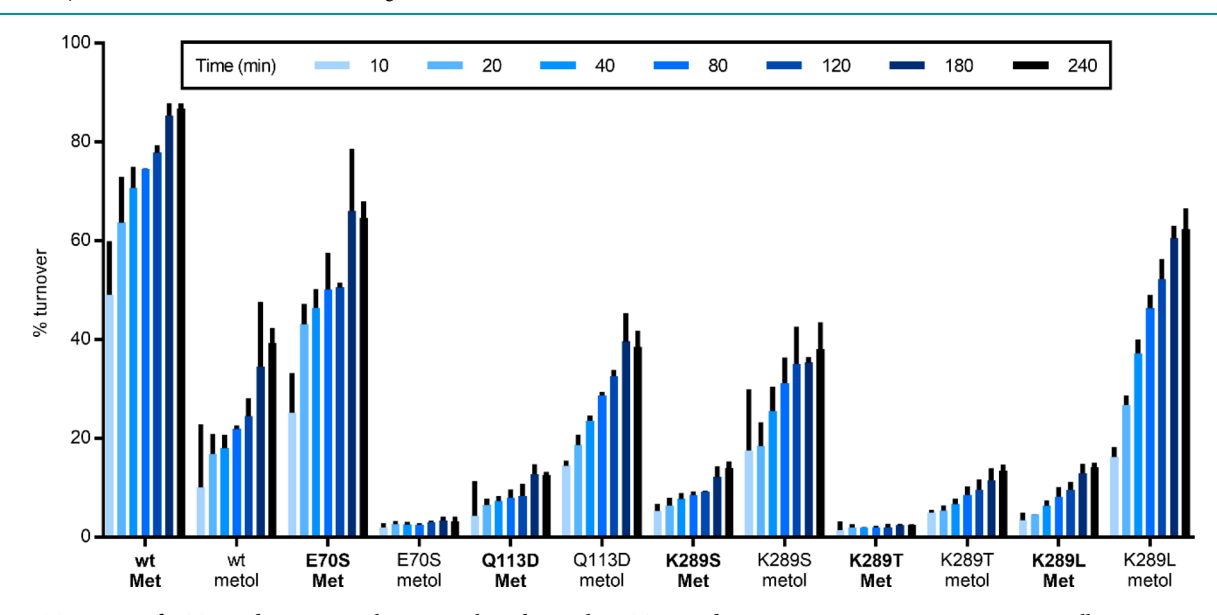


Figure 5. Turnover of ATP and Met, metol, or metolMe by wt-hMAT2A and representative mutants over time. All enzymes were at a concentration of 10 μ M in 25 mM Tris·HCl, pH 8.0, 50 mM KCl, and 10 mM MgCl₂. [Met]_i = 10 mM, [metol]_i = 10 mM, [ATP]_i = 2 mM. The mean of three independent experiments is represented by each bar, and each error bar represents \pm standard error (SEM) at 95% confidence interval (CI).

vector control, Z' = 0.44; OleD, Z' = 0.67; and hMAT2A lacking L-Met, Z' = 0.63).

Primary Screen. Using the optimized assay platform described above, 38 mutants (representing amino acid variation at four different active-site residues (E70, Q113, D258, and K289) were screened in parallel. Assays containing 5 μ L of clarified extract, 1.5 mM ATP, and 10 mM methionine analogue were incubated at 37 °C for 1 h, cooled to RT over 20 min, and then analyzed using the luciferase assay. Plate to plate standardization was based on inclusion of internal replicate positive (hMAT2A/L-Met) and negative (hMAT2A but lacking L-Met; empty vector) controls. To facilitate mutant-substrate pairing comparisons and hit selection, HT screening results were represented as the mean percent change in luminescence from the negative control (corresponding hMAT2A mutant lacking methionine analogue; Figure 4). Specifically, in this analysis, the color of each square for each hMAT2A mutant correlates to the percent change in mean relative luminescence units (RLU) among assays in the

presence or absence of a methionine analogue (where red represents increased MAT activity and blue represents decreased MAT activity compared to the negative control).

This cumulative analysis led to the following observations. First, mutation of K289 and, to a lesser extent, Q113 led to increased turnover of metol and metolMe compared to the wild-type hMAT2A conversion of these non-native surrogates. Within this context, the best substitutions at K289 included polar (Cys, Ser, and Thr), hydrophobic (Ala, Ile, Leu, Met, and Phe), or acidic (Asp and Glu) substitutions. While similar polar (Thr) or hydrophobic (Ala, Val, Ile, Leu, and Met) substitutions at Q113 provided slight improvements, acidic side chains (Asp and Glu) offered the best outcomes with metol and metolMe. Second, mutation of K289 generally led to a reduction in turnover of native substrate L-Met as exemplified by the observed outcomes with corresponding Asp, Glu, Leu, Ser, Tyr, and Val mutations. Potentially related to this catalytically important MAT K289, patients with K289N mutation in hMAT1A, an hMAT2A isoform with 84%

Table 1. Kinetic Parameters of Wild-Type hMAT2A and Mutants

hMAT2A variant	substrate ^a	$k_{\rm cat}~{\rm min}^{-1}$	$K_{ m m}~\mu{ m M}$	$k_{\rm cat}/K_{\rm m}~{\rm min}^{-1}~\mu{\rm M}^{-1}$	$k_{\mathrm{cat}}/K_{\mathrm{m}}$ relative	selectivity index ^b
wild-type	L-Met	26 ± 1.0	140 ± 50	1.9×10^{-1}	1.0	40
	L-metol	11 ± 1.6	$2,400 \pm 1,000$	4.8×10^{-3}	2.6×10^{-2}	
Q113D	L-Met	1.2 ± 0.1	47 ± 47	2.4×10^{-2}	1.0	3
	L-metol	3.3 ± 0.1	390 ± 70	8.6×10^{-3}	3.5×10^{-1}	
K289L	L-Met	0.8 ± 0.1	780 ± 170	1.1×10^{-3}	1.0	-4
	L-metol	4.1 ± 0.1	1.000 ± 130	4.1×10^{-3}	3.8	

[&]quot;Enzyme substrates were assayed in the presence of saturating ATP (2 mM). \pm standard error (SEM) at 95% confidence interval (CI). ^bFold selectivity ($k_{\rm cat}/K_{\rm m}$ L-Met divided by $k_{\rm cat}/K_{\rm m}$ L-metol) where positive values reflect preference for L-Met and negative values represent a preference for L-metol.

sequence identity, exhibit persistent hypermethioninemia. ⁹² In contrast, most mutations of Q113 had little effect on L-Met turnover. Q113, through its interaction with L-Met, is perceived as important to the closure of the hMAT2A gating loop and stabilization of the corresponding closed conformation. ⁹³ Finally, mutagenesis of D258 to His surprisingly led to nonspecific ATPase activity irrespective of L-Met or methionine surrogates employed. Consistent with this, identical assays of D258H in the absence of L-Met or a methionine surrogate revealed similar ATPase activity (Figure S4). Substitution of D258 with other amino acids was inhibitory, consistent with the strong interactions between the hMAT2A D258 side chain carboxylate and the substrate methionine alpha-amine. ^{93,94}

On the basis of the primary screen, several hMAT2A mutant and methionine analogue pairs were selected for confirmatory studies based on a perceived potential selectivity index. Namely, mutant/methionine analogue pairings were advanced if they met the following criteria: (i) reduced turnover of methionine by the mutant, (ii) reduced methionine analogue turnover with native hMAT2A, and (iii) improved turnover of the methionine analogue by the mutant (less than -35% mean change in luminescence from the negative control).

Hit Confirmation. To eliminate potential artifacts deriving from strain to strain variability in hMAT2A mutant protein levels, hit confirmation was conducted via time-course assays using fixed concentrations (10 μ M) of purified enzymes. Assays were analyzed via RP-HPLC (Figure S1), and corresponding AdoMetol or AdoMetolMe product peaks were collected and confirmed via HRMS (Figures S26 and S27). Variable protein production levels (ranging from 8.7 mg L⁻¹ for mutant K289L to 26.6 mg L⁻¹ for mutant Q113D) were observed among the test set, contributing to observed inconsistencies between the primary and secondary screens.

Key outcomes of the secondary screen are summarized in Figure 5. Under the defined time-course assay conditions, low to moderate wt-hMAT2A-catalyzed turnover of metol or racemic metolMe was observed over 240 min (39% and 17%, respectively) compared to the corresponding efficient turnover of L-Met in 10 min (49%). K289L/metol represented the best mutant-analogue combination (62% turnover in 240 min compared to 14% turnover of L-Met in 240 min), and K289L also displayed moderate efficiency with metolMe (28% in 240 min). Mutants Q113D, K289S, and K289T also displayed some selectivity toward metol (39%, 38%, and 14%, respectively; 240 min) over L-Met (13%, 14%, and 2.5%, respectively; 240 min). In contrast, K289F lacked selectivity (33% metolMe versus 30% L-Met; 240 min), while E70S lacked appreciable activity in the presence of non-native methionine surrogates (3.2% metol, 240 min versus 25% L-

Met, 10 min). Interestingly, comparative hMAT2A/mutant assays with racemic metolMe or corresponding diastereomers (*R*,*S*-metolMe or *S*,*S*-metolMe) revealed no enzymatic differentiation among metolMe stereoisomers (data not shown).

Kinetic Parameters and Non-Native AdoMet Stability. Native hMAT2A exhibited a 40-fold specificity ($k_{\rm cat}/K_{\rm m}$) preference for L-Met over metol. Conversely, mutant K289L exhibited a 4-fold specificity preference for metol over L-Met (Table 1). This analysis highlights the 17-fold difference between L-Met and metol $K_{\rm m}$ as the main contributor to substrate differentiation in hMAT2A. In contrast, a 5-fold $k_{\rm cat}$ distinction with metol versus L-Met serves as the K289L primary differentiator. Importantly, the K289L $k_{\rm cat}$ with metol (4.1 min⁻¹) is approaching that of hMAT2A with L-Met (25.7 min⁻¹), while the metol $K_{\rm m}$ of Q113D (338 μ M) is approaching the L-Met $K_{\rm m}$ of hMAT2A (138 μ M). This result may suggest there to be potential for further improvement of the bioorthogonal selectivity index via second generation mutant combinations.

A primary chemical degradation pathway of AdoMet ($t_{1/2}$ = 942 min, pH 8) occurs via intramolecular cyclization of the terminal carboxylate and the activated gamma carbon to form 5'-deoxy-5'-(methylthio)adenosine (MTA) and L-homoserine lactone (HSL). We previously demonstrated that replacing the AdoMet carboxylate with a carboxylic acid isostere prohibits this reaction and the corresponding production of MTA. ⁸³ Likewise, the conversion of AdoMetol or AdoMetolMe to MTA was not observed in any of the enzymatic reactions throughout the course of this study, even after 24 h of incubation (see Supporting Information, Figure S1). This AdoMetol/AdoMetolMe chemical stability may present unique advantages in the context of future intracellular bioothorgonal applications.

K289L Three-Dimensional Structure. Sites were chosen for mutagenesis by analysis of the binding pocket interactions of the side chains with the SAM amino acid backbone from the previous crystal structure. Specifically, E70, Q113, D258, and K289 were selected for mutation because of their electrostatic interactions with SAM in the binding pocket (Figure 2A). Of the array of mutants evaluated, K289L was found to provide the greatest shift in selectivity toward non-native substrates metol and metolMe with a concomitant notable reduction of turnover of the native substrate L-Met. To assess the impact of the K289 mutation on the overall hMAT2A three-dimensional structure and improved non-native substrate ligand interactions, we solved the structure of the hMAT2A mutant K289L to a nominal resolution of 2.3 Å (PDB: 6P9V). The determined K289L structure confirmed conservation of wildtype overall fold and conformation and the intended alteration of binding pocket electrostatics. The observed K289L substrate

binding pocket changes were subtle with a water replacing the wild-type K289 side chain amine. Unfortunately, all attempts to obtain crystals in the presence of the non-native substrate (L-metol) were unsuccessful due to ADP degradation over the six month crystal growth period that was required to obtain these crystals. The final model contains residues 16–395 of the protein, an adenosine, one magnesium, and one potassium ion, in disordered density adjacent to the metal binding site that was interpreted as pyrophosphate and 148 water molecules. The first 35 residues of the N-terminus were disordered and were not modeled. For X-ray diffraction statistics and binding pocket density, see Supporting Information Table S1 and Supporting Information Figure S3, respectively.

Conclusions. In summary, this study highlights the first example of exchanging L-Met terminal carboxylate/amine recognition elements within the hMAT2A active-site to enable non-native bioorthogonal substrate utilization (Figure 1D). As many AdoMet-producing (e.g., hMAT2A) and AdoMetutlizing (e.g., MTs) enzymes adopt similar active-site strategies for substrate recognition, 93-97 the proof of concept first generation hMAT2A engineering highlighted herein is expected to translate to a range of AdoMet-utilizing target enzymes. Importantly, the new conceptual design put forth affords two distinct advantages over previously reported innovative bioorthogonal strategies for AdoMet production/ utilization (Figure 1B and C). First, unlike strategies that rely on MAT/MT engineering to accommodate additional steric bulk of specific S-alkyl substitutions (e.g., the S-butynyl AdoMet analogue-based approach reported by Klimašauskas and co-workers or the coupled S-(E)-hex-2-en-5-ynyl L-Met/ AdoMet analogue-based platform reported by Luo and colleagues; 59,60,98 Figure 1B), the current strategy does not rely on specific substrate S-alkyl substitutions as a bioorthogonal differentiator and is thereby anticipated to afford greater flexibility in the S-alkyl "tags" that can be employed. Second, in contrast to all previously reported L-Met/AdoMet platforms (Figure 1B and C), 7699-101 the current strategy's replacement of L-Met/AdoMet terminal nucleophilic carboxylate as the bioothogonal recognition element provides uniquely stable AdoMet reagents for biochemical or intracellular studies.

On the basis of comparative kinetic parameters, the first generation hMAT2A engineering strategy highlighted herein led to a 160-fold inversion of the hMAT2A selectivity index (from 40-fold L-Met/metol bias for hMAT2A to a 4-fold metol/L-Met preference for K289L). This compares favorably to previously reported bioorthogonal engineering approaches to AdoMet-producing/utlizing enzymes. For example, Schultz and Gray reported a 260-fold inversion of the selectivity index as the first application of "bump-and-hole" engineering principles to a protein arginine MT (Rmt1) via a designed E117G mutant to accommodate a nucleoside N6-benzylmodified AdoMet analogue. 82 A subsequent M. HhaI DNA cytosine-5 MT Y254S/N304A double mutant, designed by Klimašauskas and co-workers to pair with S-butynyl AdoMet, led to a 24-fold increase in turnover with the non-native substrate based on comparative end point assays. 98 In the most recent published example, Luo and colleagues noted a 30-50fold selectivity preference using an S-(E)-hex-2-en-5-ynyl L-Met analogue in an engineered MAT (hMAT2A I117A)chromatin-modifying protein MT (G9a Y1154A) coupled reaction based on 30-50-fold enrichment of chromatin DNA (compared to control group transfected with hMAT2A I117A mutant alone). 59,60 While these cumulative studies highlight

the ability to engineer non-native substrate selectivity of representative enzymes, the rules regarding the selectivity magnituge and/or mechanism (i.e., $k_{\rm cat}$ -driven versus $K_{\rm m}$ -driven) required for suitable cell-based bioorthogonality have yet to be established. The availability of well-characterized systems with variable selectivities (such as the MAT variants described herein) are anticipated to enable a more systematic analysis of the minimal requirements for successful translation to cell-based applications.

METHODS

Preparation of Mutant Library. The pET28a-hMAT2A plasmid used for heterologous hMAT2A production and as the template DNA for all site-directed mutagenesis PCR reactions was previously reported. 65,66,83 Mutants were generated using the QuikChange II kit (Agilent Technologies, Santa Clara, CA) according to the manufacturer's instructions. Mutagenic primers were designed using the online QuikChange Primer Design software (www.genomics. agilent.com) and are listed in Table S1. Following mutagenesis reactions, an aliquot (1 μ L) of each reaction was transformed into chemically competent *E. coli* XL-1 Blue cells (provided in QuikChange II kit) following the manufacturer's directions. The transformation mixture was plated on LB-agar plates containing 50 μ g mL $^{-1}$ of kanamycin and incubated at 37 °C for 18 h.

DNA Analysis and Sequencing. Single colonies from mutagenic transformations (above) were individually cultured via standard protocols, and corresponding mutant plasmid DNA was isolated from each cultured strain using the QIAprep Spin Miniprep kit (QIAGEN GmbH, Hilden, Germany). Glycerol stocks of each colony were made by mixing equal volume cultures with 50% (v/v) glycerol and storing them at $-80\,^{\circ}\text{C}$. Mutants were sequence confirmed via forward and reverse sequencing. All DNA sequencing was performed by ACGT, Inc. (Wheeling, IL) with T7 promoter (5'-TAATACGACT-CACTATAGGG) and T7 terminator (5'-GCTAGTTATT-GCTCAGCGG) primers.

Library Transformation. Leftover plasmid DNA encoding each desired mutation was transformed into chemically competent E. coli BL21(DE3) cells (New England Biolabs, Ipswich, MA) following the manufacturer's protocol and plated on LB-agar plates supplemented with 50 μg mL⁻¹ kanamycin. Individual colonies selected from corresponding plates grown overnight were used to inoculate wells of a 96-deep-well microtiter plate (Corning Costar Assay Block, 2 mL, 96 Well, Square V-Bottom; Corning, NY) in which each well contained 1 mL of LB medium supplemented with 50 µg mL⁻¹ kanamycin. Culture plates were tightly sealed with AeraSeal breathable film (Excel Scientific, Inc., Victorville, CA). After cell growth at 37 °C for 18 h with shaking at 325 rpm, a glycerol copy was made via addition of 1 mL of 50% (v/v) glycerol. The master glycerol stock plate was tightly sealed with TempPlate sealing foil (USA Scientific, Inc., Ocala, FL) and stored at -80 °C. Each 96-well culture plate contained two copies of each mutant-expressing construct, eight copies each of wild-type hMAT2A and empty pET28a constructs, and two sterile wells.

Protein Production. A 96-deep-well microtiter plate containing 1 mL of LB medium supplemented with 50 μ g mL⁻¹ kanamycin was inoculated from the master glycerol stock plate. Culture plates were tightly sealed with AeraSeal breathable film. After cell growth at 37 °C for 18 h with shaking at 325 rpm, 100 μ L of each culture was transferred to a fresh deep-well plate containing 1 mL of LB medium supplemented with 50 μ g mL⁻¹ kanamycin. The freshly inoculated plate was incubated at 37 °C for 1 h 45 min with shaking at 325 rpm. N-terminal His₆-tagged hMAT2A gene transcription was induced at an optical cell density (OD₆₀₀) of ~0.7 *via* the addition of isopropyl β-D-1-thiogalactopyranoside (IPTG, final concentration 0.5 mM), and the plate was incubated for 18 h at 18 °C with shaking at 325 rpm. Cells were harvested by centrifugation at 3000g for 20 min at 4 °C. Each cell pellet was thoroughly resuspended in 50 μ L of 25 mM Tris-HCl (pH 8.0) containing 10 mM MgCl₂, 50 mM KCl, and 10 mg

 $\rm mL^{-1}$ lysozyme (Millipore Sigma) at 4 °C; transferred to a 96-well full-skirt PCR plate (TempPlate, USA Scientific, Inc.); sealed with TempPlate sealing foil; and subjected to a single freeze—thaw cycle to lyse the cells. Cell debris was then collected by centrifugation at 3000g for 20 min at 4 °C, and the cleared supernatant was used for enzyme assays.

Library Screening. In a white 384-well plate (OptiPlate, PerkinElmer, Inc., Waltham, MA), 5 μ L of cleared supernatant was mixed with an equal volume (5 μ L) of 25 mM Tris·HCl (pH 8.0) containing 10 mM MgCl₂, 50 mM KCl, 20 mM L-Met (or methionine surrogate), and 3.0 mM ATP using a VIAFLO 96 hand-held 96-channel pipet (INTEGRA Biosciences Corp., Hudson, NH). Upon mixing, the plates were tightly sealed with sealing foil, and the reactions were incubated at 37 °C for 1 h and cooled to RT over 20 min. After the reactions were equilibrated to RT, each reaction was mixed with an equal volume (10 μ L) of Kinase-Glo Max reagent (Promega Corporation, Madison, WI) previously also equilibrated to RT. The assay plate was incubated for 10 min at RT and luminescence subsequently measured using a FLUOstar Omega plate reader (BMG LABTECH GmbH, Offenburg, Germany).

In Vitro Time-Course Assays (Hit Confirmation). In vitro hMAT2A mutant reactions were conducted at a volume of 100 µL with saturating ATP (2 mM) and methionine or methionine analogue (10 mM), 10 μ M purified mutant or wt-hMAT2A in 25 mM Tris, at pH 8.0, 10 mM MgCl₂, and 50 mM KCl. Reactions were incubated at 37 °C, and 20 μ L aliquots were taken at various time intervals (10, 20, 40, 80, 120, 180, and 240 min) and quenched with equal volumes of MeOH followed by centrifugation (10 000g, 20 min) to remove the precipitated protein. Product formation for each reaction was subsequently analyzed by RP-HPLC (see Supporting Information, Figure S1). For each reaction, product (AdoMet, AdoMetol, or AdoMetolMe) concentration was based on the integration of species at 260 nm and calculated by multiplying the initial concentration of ATP by the quotient of the integrated product (AdoMet plus MTA, AdoMetol, or AdoMetolMe) HPLC peak area (mAU*sec) over the sum of the integrated peak areas for the product and remaining ATP as previously reported. 65,66,83 MTA derives from AdoMet and was thereby also considered as contributing to the total product concentration. Assays were repeated in triplicate, and Figure 5 represents an average of replicates. Controls lacking enzyme, methionine, metol, metolMe, and/or ATP led to no product.

In Vitro Kinetic Assays. To determine the K_m and k_{cat} of select hMAT2A mutants with L-Met and/or analogues thereof, in vitro hMAT2A mutant reactions were conducted in a volume of 50 μ L with saturating ATP (2 mM), varied concentrations of L-Met or analogues thereof (0.3-12 mM), 10 µM purified mutant or wt-hMAT2A in 25 mM Tris, at pH 8.0, 10 mM MgCl₂, and 50 mM KCl. Reactions were incubated at 37 °C and subsequently quenched, while the reactions still exhibited linear kinetics per the reaction progress curves (Figure 5), by adding an equal volume of MeOH followed by centrifugation (10 000g, 20 min) to remove the precipitated protein. Product formation for each reaction was subsequently analyzed by RP-HPLC as described in the preceding section (see Supporting Information, Figure S1). Assays were repeated in triplicate where the Michaelis-Menten plots in Figure S2 represent an average of replicates. Controls lacking enzyme, methionine, metol, metolMe, and/or ATP led to no product.

ASSOCIATED CONTENT

Supporting Information

The Supporting Information is available free of charge at https://pubs.acs.org/doi/10.1021/acschembio.9b00943.

Additional materials and methods and supplementary data tables and figures (PDF)

AUTHOR INFORMATION

Corresponding Authors

George N. Phillips, Jr. – Department of Biosciences and Department of Chemistry, Rice University, Houston, Texas 77251-1892, United States; Phone: (713) 348-6951; Email: georgep@rice.edu

Jon S. Thorson — Department of Pharmaceutical Sciences, College of Pharmacy and Center for Pharmaceutical Research and Innovation (CPRI), College of Pharmacy, University of Kentucky, Lexington, Kentucky 40536-0596, United States; orcid.org/0000-0002-7148-0721; Phone: (859) 218-0140; Email: jsthorson@uky.edu

Authors

Tyler D. Huber – Department of Pharmaceutical Sciences, College of Pharmacy and Center for Pharmaceutical Research and Innovation (CPRI), College of Pharmacy, University of Kentucky, Lexington, Kentucky 40536-0596, United States

Jonathan A. Clinger – Department of Biosciences, Rice University, Houston, Texas 77251-1892, United States

Yang Liu – Department of Pharmaceutical Sciences, College of Pharmacy and Center for Pharmaceutical Research and Innovation (CPRI), College of Pharmacy, University of Kentucky, Lexington, Kentucky 40536-0596, United States

Weijun Xu – Department of Biosciences, Rice University, Houston, Texas 77251-1892, United States

Mitchell D. Miller – Department of Biosciences, Rice University, Houston, Texas 77251-1892, United States

Complete contact information is available at: https://pubs.acs.org/10.1021/acschembio.9b00943

Notes

The authors declare the following competing financial interest(s): J.S.T. is a co-founder of Centrose (Madison, WI).

ACKNOWLEDGMENTS

This work was supported in part by NIH R01 GM115261 (J.S.T. and G.N.P.), the NIH Protein Structure Initiative (U01 GM098248, G.N.P.), NIH GM109456 (G.N.P.), NIH T32 GM008280 (J.A.C.), the University of Kentucky College of Pharmacy, the National Center for Advancing Translational Sciences (UL1TR000117 and UL1TR001998), and the National Science Foundation BioXFEL STC (1231306; G.N.P.). We also thank the University of Kentucky Mass Spectrometry Facility (ASTeCC) for HRMS support and the staff at the LS-CAT and GM/CA beamline at the Advanced Photo Source for help in conducting trial attempts and collecting the diffraction data. This research used resources of the Advanced Photon Source, a U.S. Department of Energy (DOE) Office of Science User Facility operated for the DOE Office of Science by Argonne National Laboratory under Contract No. DE-AC02-06CH11357. Use of LS-CAT Sector 21 was supported by the Michigan Economic Development Corporation and the Michigan Technology Tri-Corridor (Grant 085P1000817). GM/CA@APS has been funded in whole or in part with Federal funds from the National Cancer Institute (ACB-12002) and the National Institute of General Medical Sciences (AGM-12006).

REFERENCES

(1) Struck, A.-W., Thompson, M. L., Wong, L. S., and Micklefield, J. (2012) S-Adenosyl-methionine-dependent methyltransferases: Highly

versatile enzymes in biocatalysis, biosynthesis and other biotechnological applications. *ChemBioChem 13*, 2642–2655.

- (2) Westfall, C. S., Muehler, A. M., and Jez, J. M. (2013) Enzyme action in the regulation of plant hormone responses. *J. Biol. Chem.* 288, 19304–19311.
- (3) Wessjohann, L. A., Keim, J., Weigel, B., and Dippe, M. (2013) Alkylating enzymes. Curr. Opin. Chem. Biol. 17, 229-235.
- (4) Vance, D. E. (2014) Phospholipid methylation in mammals: From biochemistry to physiological function. *Biochim. Biophys. Acta, Biomembr.* 1838, 1477–1487.
- (5) Liscombe, D. K., Louie, G. V., and Noel, J. P. (2012) Architectures, mechanisms and molecular evolution of natural product methyltransferases. *Nat. Prod. Rep.* 29, 1238–1250.
- (6) Klimašauskas, S., and Weinhold, E. (2007) A new tool for biotechnology: AdoMet-dependent methyltransferases. *Trends Biotechnol.* 25, 99–104.
- (7) Arrowsmith, C. H., Bountra, C., Fish, P. V., Lee, K., and Schapira, M. (2012) Epigenetic protein families: A new frontier for drug discovery. *Nat. Rev. Drug Discovery* 11, 384–400.
- (8) Chen, B. F., and Chan, W. Y. (2014) The de novo DNA methyltransferase DNMT3A in development and cancer. *Epigenetics* 9, 669–677.
- (9) Dong, H., Fink, K., Züst, R., Lim, S. P., Qin, C. F., and Shi, P. Y. (2014) Flavivirus RNA methylation. *J. Gen. Virol.* 95, 763–778.
- (10) Urbonavičius, J., Meškys, R., and Grosjean, H. (2014) Biosynthesis of wyosine derivatives in tRNA^{Phe} of Archaea: Role of a remarkable bifunctional tRNA^{Phe}:m¹G/imG2 methyltransferase. RNA 20, 747–753.
- (11) Lanouette, S., Mongeon, V., Figeys, D., and Couture, J.-F. (2014) The functional diversity of protein lysine methylation. *Mol. Syst. Biol.* 10, 724–724.
- (12) Yamamoto, T., Takano, N., Ishiwata, K., Ohmura, M., Nagahata, Y., Matsuura, T., Kamata, A., Sakamoto, K., Nakanishi, T., Kubo, A., Hishiki, T., and Suematsu, M. (2014) Reduced methylation of PFKFB3 in cancer cells shunts glucose towards the pentose phosphate pathway. *Nat. Commun.* 5, 3480.
- (13) Bottiglieri, T. (2002) S-Adenosyl-L-methionine (SAMe): from the bench to the bedside—Molecular basis of a pleiotrophic molecule. *Am. J. Clin. Nutr.* 76, 1151S—1157S.
- (14) Cacabelos, R. (2014) Epigenomic networking in drug development: from pathogenic mechanisms to pharmacogenomics. *Drug Dev. Res.* 75, 348–365.
- (15) Lu, S. C., and Mato, J. M. (2012) S-Adenosylmethionine in liver health, injury, and cancer. *Physiol. Rev.* 92, 1515–1542.
- (16) Campbell, R. M., and Tummino, P. J. (2014) Cancer epigenetics drug discovery and development: The challenge of hitting the mark. *J. Clin. Invest.* 124, 64–69.
- (17) Gapp, K., Woldemichael, B. T., Bohacek, J., and Mansuy, I. M. (2014) Epigenetic regulation in neurodevelopment and neurodegenerative diseases. *Neuroscience* 264, 99–111.
- (18) Tremolizzo, L., Rodriguez-Menendez, V., Conti, E., Zoia, C., Cavaletti, G., and Ferrarese, C. (2014) Novel therapeutic targets in neuropsychiatric disorders: The neuroepigenome. *Curr. Pharm. Des.* 20, 1831–1839.
- (19) Coşar, A., Ipçioğlu, O. M., Özcan, Ö., and Gültepe, M. (2014) Folate and homocysteine metabolisms and their roles in the biochemical basis of neuropsychiatry. *Turk. J. Med. Sci.* 44, 1–9.
- (20) Grolleau-Julius, A., Ray, D., and Yung, R. L. (2010) The role of epigenetics in aging and autoimmunity. *Clin. Rev. Allergy Immunol.* 39, 42–50.
- (21) Doyle, H. A., Yang, M.-L., Raycroft, M. T., Gee, R. J., and Mamula, M. J. (2014) Autoantigens: Novel forms and presentation to the immune system. *Autoimmunity* 47, 220–233.
- (22) Vickers, M. H. (2014) Early life nutrition, epigenetics and programming of later life disease. *Nutrients* 6, 2165–2178.
- (23) Wang, T., Warren, S. T., and Jin, P. (2013) Toward pluripotency by reprogramming: Mechanisms and application. *Protein Cell* 4, 820–832.

- (24) Hu, K. (2014) All roads lead to induced pluripotent stem cells: The technologies of iPSC generation. Stem Cells Dev. 23, 1285–300.
- (25) Balmer, N. V., and Leist, M. (2014) Epigenetics and transcriptomics to detect adverse drug effects in model systems of human development. *Basic Clin. Pharmacol. Toxicol.* 115, 59–68.
- (26) Khan, S. R., Baghdasarian, A., Fahlman, R. P., Michail, K., and Siraki, A. G. (2014) Current status and future prospects of toxicogenomics in drug discovery. *Drug Discovery Today* 19, 562–578.
- (27) Lötsch, J., Schneider, G., Reker, D., Parnham, M. J., Schneider, P., Geisslinger, G., and Doehring, A. (2013) Common non-epigenetic drugs as epigenetic modulators. *Trends Mol. Med.* 19, 742–753.
- (28) Bonnin, R. A, Nordmann, P., and Poirel, L. (2013) Screening and deciphering antibiotic resistance in *Acinetobacter baumannii*: A state of the art. *Expert Rev. Anti-Infect. Ther.* 11, 571–583.
- (29) Wang, R., and Luo, M. (2013) A journey toward bioorthogonal profiling of protein methylation inside living cells. *Curr. Opin. Chem. Biol.* 17, 729–737.
- (30) Luo, M. (2012) Current chemical biology approaches to interrogate protein methyltransferases. ACS Chem. Biol. 7, 443–463.
- (31) Schapira, M., Jin, J., Barsyte-Lovejoy, D., Li, F., Kaniskan, H. Ü., Northrop, J. P., Brown, P. J., McLeod, D., Arrowsmith, C. H., De Carvalho, D. D., Liu, J., Shen, Y., Scheer, S., Ackloo, S., Zaph, C., Medina, T. S., Lewis, A. M., Zepeda-Velazquez, C. A., Vedadi, M., Luo, M., Smil, D., Ward, J. A., Richardson, P. L., and Huber, K. V. M. (2019) A chemical biology toolbox to study protein methyltransferases and epigenetic signaling. *Nat. Commun.* 10, 1–14.
- (32) Hartstock, K., and Rentmeister, A. (2019) Mapping N⁶-methyladenosine (m⁶A) in RNA: Established methods, remaining challenges, and emerging approaches. *Chem. Eur. J.* 25, 3455–3464.
- (33) Bennett, M. R., Shepherd, S. A., Cronin, V. A., and Micklefield, J. (2017) Recent advances in methyltransferase biocatalysis. *Curr. Opin. Chem. Biol.* 37, 97–106.
- (34) Pljevaljcić, G., Pignot, M., and Weinhold, E. (2003) Design of a new fluorescent cofactor for DNA methyltransferases and sequence-specific labeling of DNA. *J. Am. Chem. Soc.* 125, 3486–3492.
- (35) Pljevaljcić, G., Schmidt, F., and Weinhold, E. (2004) Sequence-specific methyltransferase-induced labeling of DNA (SMILing DNA). *ChemBioChem* 5, 265–269.
- (36) Zhang, C., Weller, R. L., Thorson, J. S., and Rajski, S. R. (2006) Natural product diversification using a non-natural cofactor analogue of S-adenosyl-L-methionine. *J. Am. Chem. Soc.* 128, 2760–2761.
- (37) Gottfried, A., and Weinhold, E. (2011) Sequence-specific covalent labelling of DNA. *Biochem. Soc. Trans.* 39, 623–628.
- (38) Lukinavičius, G., Lapienė, V., Staševskij, Z., Dalhoff, C., Weinhold, E., and Klimašauskas, S. (2007) Targeted labeling of DNA by methyltransferase-directed transfer of activated groups (mTAG). *J. Am. Chem. Soc.* 129, 2758–2759.
- (39) Dalhoff, C., Lukinavičius, G., Klimasauskas, S., and Weinhold, E. (2006) Direct transfer of extended groups from synthetic cofactors by DNA methyltransferases. *Nat. Chem. Biol.* 2, 31–32.
- (40) Schulz, D., Holstein, J. M., and Rentmeister, A. (2013) A chemo-enzymatic approach for site-specific modification of the RNA cap. *Angew. Chem., Int. Ed.* 52, 7874–7878.
- (41) Holstein, J. M., Stummer, D., and Rentmeister, A. (2015) Engineering *Giardia lamblia* trimethylguanosine synthase (GlaTgs2) to transfer non-natural modifications to the RNA 5'-cap. *Protein Eng., Des. Sel.* 28, 179–186.
- (42) McCoy, L. S., Shin, D., and Tor, Y. (2014) Isomorphic emissive GTP surrogate facilitates initiation and elongation of in vitro transcription reactions. *J. Am. Chem. Soc.* 136, 15176–15184.
- (43) Holstein, J. M., Stummer, D., and Rentmeister, A. (2016) Enzymatic modification of 5'-capped RNA and subsequent labeling by click chemistry. *Methods Mol. Biol.* 1428, 45–60.
- (44) Holstein, J. M., Muttach, F., Schiefelbein, S. H. H., and Rentmeister, A. (2017) Dual 5'cap labeling based on regioselective RNA methyltransferases and bioorthogonal reactions. *Chem. Eur. J.* 23, 6165–6173.
- (45) Muttach, F., Mäsing, F., Studer, A., and Rentmeister, A. (2017) New AdoMet analogues as tools for enzymatic transfer of photo-

cross-linkers and capturing RNA-protein interactions. Chem. - Eur. J. 23, 5988-5993.

- (46) Holstein, J. M., Anhäuser, L., and Rentmeister, A. (2016) Modifying the 5'-cap for click reactions of eukaryotic mRNA and to tune translation efficiency in living Cells. *Angew. Chem., Int. Ed.* 55, 10899–10903.
- (47) Holstein, J. M., Stummer, D., and Rentmeister, A. (2015) Enzymatic modification of 5'-capped RNA with a 4-vinylbenzyl group provides a platform for photoclick and inverse electron-demand Diels-Alder reaction. *Chem. Sci.* 6, 1362–1369.
- (48) Heimes, M., Kolmar, L., and Brieke, C. (2018) Efficient cosubstrate enzyme pairs for sequence-specific methyltransferase-directed photolabile caging of DNA. *Chem. Commun.* 54, 12718–12721.
- (49) Tomkuviene, M., Clouet-d'Orval, B., Černiauskas, I., Weinhold, E., and Klimašauskas, S. (2012) Programmable sequence-specific click-labeling of RNA using archaeal box C/D RNP methyltransferases. *Nucleic Acids Res.* 40, 6765–6773.
- (50) Neely, R. K., Dedecker, P., Hotta, J., Urbanaviciute, G., Klimasauskas, S., and Hofkens, J. (2010) DNA fluorocode: A single molecule, optical map of DNA with nanometre resolution. *Chem. Sci.* 1, 453–460.
- (51) Ibáñez, G., McBean, J. L., Astudillo, Y. M., and Luo, M. (2010) An enzyme-coupled ultrasensitive luminescence assay for protein methyltransferases. *Anal. Biochem.* 401, 203–210.
- (52) Islam, K., Zheng, W., Yu, H., Deng, H., and Luo, M. (2011) Expanding cofactor repertoire of protein lysine methyltransferase for substrate labeling. ACS Chem. Biol. 6, 679–684.
- (53) Islam, K., Bothwell, I., Chen, Y., Sengelaub, C., Wang, R., Deng, H., and Luo, M. (2012) Bioorthogonal profiling of protein methylation using azido derivative of S-adenosyl-L-methionine. *J. Am. Chem. Soc.* 134, 5909–5915.
- (54) Ibáñez, G., Shum, D., Blum, G., Bhinder, B., Radu, C., Antczak, C., Luo, M., and Djaballah, H. (2012) A high throughput scintillation proximity imaging assay for protein methyltransferases. *Comb. Chem. High Throughput Screening* 15, 359–371.
- (55) Wang, R., Zheng, W., Yu, H., Deng, H., and Luo, M. (2011) Labeling substrates of protein arginine methyltransferase with engineered enzymes and matched S-adenosyl-L-methionine analogues. J. Am. Chem. Soc. 133, 7648–7651.
- (56) Blum, G., Islam, K., and Luo, M. (2013) Bioorthogonal profiling of protein methylation (BPPM) using an azido analog of S-Adenosyl-L-methionine, in *Current Protocols in Chemical Biology*, pp 45–66, John Wiley & Sons, Inc., Hoboken, NJ.
- (57) Bothwell, I. R., Islam, K., Chen, Y., Zheng, W., Blum, G., Deng, H., and Luo, M. (2012) Se-Adenosyl-L-selenomethionine cofactor analogue as a reporter of protein methylation. J. Am. Chem. Soc. 134, 14905–14912.
- (58) Sohtome, Y., Shimazu, T., Barjau, J., Fujishiro, S., Akakabe, M., Terayama, N., Dodo, K., Ito, A., Yoshida, M., Shinkai, Y., and Sodeoka, M. (2018) Unveiling epidithiodiketopiperazine as a non-histone arginine methyltransferase inhibitor by chemical protein methylome analyses. *Chem. Commun.* 54, 9202.
- (59) Islam, K., Chen, Y., Wu, H., Bothwell, I. R., Blum, G. J., Zeng, H., Dong, A., Zheng, W., Min, J., Deng, H., and Luo, M. (2013) Defining efficient enzyme-cofactor pairs for bioorthogonal profiling of protein methylation. *Proc. Natl. Acad. Sci. U. S. A. 110*, 16778–16783.
- (60) Wang, R., Islam, K., Liu, Y., Zheng, W., Tang, H., Lailler, N., Blum, G., Deng, H., and Luo, M. (2013) Profiling genome-wide chromatin methylation with engineered posttranslation apparatus within living cells. *J. Am. Chem. Soc.* 135, 1048–1056.
- (61) Struck, A.-W., Bennett, M. R., Shepherd, S. A., Law, B. J. C., Zhuo, Y., Wong, L. S., and Micklefield, J. (2016) An enzyme cascade for selective modification of tyrosine residues in structurally diverse peptides and proteins. *J. Am. Chem. Soc.* 138, 3038–3045.
- (62) Zhang, Y., Pan, Y., Liu, W., Zhou, Y. J., Wang, K., Wang, L., Sohail, M., Ye, M., Zou, H., and Zhao, Z. K. (2016) In vivo protein allylation to capture protein methylation candidates. *Chem. Commun.* 52, 6689–6692.

- (63) Peters, W., Willnow, S., Duisken, M., Kleine, H., Macherey, T., Duncan, K. E., Litchfield, D. W., Lüscher, B., and Weinhold, E. (2010) Enzymatic site-specific functionalization of protein methyltransferase substrates with alkynes for click labeling. *Angew. Chem., Int. Ed.* 49, 5170–5173.
- (64) Binda, O., Boyce, M., Rush, J. S., Palaniappan, K. K., Bertozzi, C. R., and Gozani, O. (2011) A chemical method for labeling lysine methyltransferase substrates. *ChemBioChem* 12, 330–334.
- (65) Singh, S., Zhang, J., Huber, T. D., Sunkara, M., Hurley, K., Goff, R. D., Wang, G., Zhang, W., Liu, C., Rohr, J., Van Lanen, S. G., Morris, A. J., and Thorson, J. S. (2014) Facile chemoenzymatic strategies for the synthesis and utilization of S-adenosyl-L-methionine analogues. *Angew. Chem., Int. Ed.* 53, 3965–3969.
- (66) Wang, F., Singh, S., Zhang, J., Huber, T. D., Helmich, K. E., Sunkara, M., Hurley, K. A., Goff, R. D., Bingman, C. A., Morris, A. J., Thorson, J. S., and Phillips, G. N. (2014) Understanding molecular recognition of promiscuity of thermophilic methionine adenosyltransferase sMAT from *Sulfolobus solfataricus*. *FEBS J.* 281, 4224–4239
- (67) Stecher, H., Tengg, M., Ueberbacher, B. J., Remler, P., Schwab, H., Griengl, H., and Gruber-Khadjawi, M. (2009) Biocatalytic Friedel-Crafts alkylation using non-natural cofactors. *Angew. Chem.* 121, 9710–9712.
- (68) Law, B. J. C., Struck, A.-W., Bennett, M. R., Wilkinson, B., and Micklefield, J. (2015) Site-specific bioalkylation of rapamycin by the RapM 16-O-methyltransferase. *Chem. Sci.* 6, 2885–2892.
- (69) Winter, J. M., Chiou, G., Bothwell, I. R., Xu, W., Garg, N. K., Luo, M., and Tang, Y. (2013) Expanding the structural diversity of polyketides by exploring the cofactor tolerance of an inline methyltransferase domain. *Org. Lett.* 15, 3774.
- (70) Lee, B. W. K., Sun, H. G., Zang, T., Kim, B. J., Alfaro, J. F., and Zhou, Z. S. (2010) Enzyme-catalyzed transfer of a ketone group from an S-adenosylmethionie analog: A tool for the functional analysis of methyltransferases. *J. Am. Chem. Soc.* 132, 3642–3643.
- (71) Bishop, A. C., Kung, C., Shah, K., Witucki, L., Shokat, K. M., and Liu, Y. (1999) Generation of monospecific nanomolar tyrosine kinase inhibitors via a chemical genetic approach. *J. Am. Chem. Soc.* 121, 627–631.
- (72) Ubersax, J. A., Woodbury, E. L., Quang, P. N., Paraz, M., Blethrow, J. D., Shah, K., Shokat, K. M., and Morgan, D. O. (2003) Targets of the cyclin-dependent kinase Cdk1. *Nature* 425, 859–864.
- (73) Bishop, A. C., Shah, K., Liu, Y., Witucki, L., Kung, C., and Shokat, K. M. (1998) Design of allele-specific inhibitors to probe protein kinase signaling. *Curr. Biol.* 8, 257–266.
- (74) Guo, Z., Zhou, D., and Schultz, P. G. (2000) Designing small-molecule switches for protein-protein interactions. *Science (Washington, DC, U. S.)* 288, 2042–2045.
- (75) Belshaw, P. J., Schoepfer, J. G., Liu, K.-Q., Morrison, K. L., and Schreiber, S. L. (1995) Rational design of orthogonal receptor—ligand combinations. *Angew. Chem., Int. Ed. Engl.* 34, 2129—2132.
- (76) Islam, K. (2018) The bump-and-hole tactic: Expanding the scope of chemical genetics. *Cell Chem. Biol.* 25, 1171–1184.
- (77) Islam, K. (2015) Allele-specific chemical genetics: Concept, strategies, and applications. ACS Chem. Biol. 10, 343–363.
- (78) Shokat, K. M. (1995) Tyrosine kinases: Modular signaling enzynes with tunable specificities. *Chem. Biol.* 2, 509–514.
- (79) Bishop, A., Buzko, O., Heyeck-Dumas, S., Jung, I., Kraybill, B., Liu, Y., Shah, K., Ulrich, S., Witucki, L., Yang, F., Zhang, C., and Shokat, K. M. (2000) Unnatural ligands for engineered proteins: new tools for chemical genetics. *Annu. Rev. Biophys. Biomol. Struct.* 29, 577–606.
- (80) Vranken, C., Deen, J., Dirix, L., Stakenborg, T., Dehaen, W., Leen, V., Hofkens, J., and Neely, R. K. (2014) Super-resolution optical DNA mapping via DNA methyltransferase-directed click chemistry. *Nucleic Acids Res.* 42, No. e50.
- (81) Motorin, Y., Burhenne, J., Teimer, R., Koynov, K., Willnow, S., Weinhold, E., and Helm, M. (2011) Expanding the chemical scope of RNA:methyltransferases to site-specific alkynylation of RNA for click labeling. *Nucleic Acids Res.* 39, 1943–1952.

- (82) Lin, Q., Jiang, F., Schultz, P. G., and Gray, N. S. (2001) Design of allele-specific protein methyltransferase inhibitors. *J. Am. Chem. Soc.* 123, 11608–11613.
- (83) Huber, T. D., Wang, F., Singh, S., Johnson, B. R., Zhang, J., Sunkara, M., Van Lanen, S. G., Morris, A. J., Phillips, G. N., Jr., and Thorson, J. S. (2016) Functional AdoMet isosteres resistant to classical AdoMet degradation pathways. *ACS Chem. Biol.* 11, 2484–2491.
- (84) Thomsen, M., Vogensen, S. B., Buchardt, J., Burkart, M. D., and Clausen, R. P. (2013) Chemoenzymatic synthesis and in situ application of S-adenosyl-L-methionine analogs. *Org. Biomol. Chem.* 11, 7606–7610.
- (85) Iwig, D. F., and Booker, S. J. (2004) Insight into the polar reactivity of the onium chalcogen analogues of S-adenosyl-L-methionine. *Biochemistry* 43, 13496–13509.
- (86) Hoffman, J. L. (1986) Chromatographic analysis of the chiral and covalent instability of S-adenosyl-L-methionine. *Biochemistry* 25, 4444–4449.
- (87) Bentley, R. (2005) Role of sulfur chirality in the chemical processes of biology. *Chem. Soc. Rev.* 34, 609-624.
- (88) Yaginuma, H., Kawai, S., Tabata, K. V., Tomiyama, K., Kakizuka, A., Komatsuzaki, T., Noji, H., and Imamura, H. (2015) Diversity in ATP concentrations in a single bacterial cell population revealed by quantitative single-cell imaging. *Sci. Rep. 4*, 6522.
- (89) Zhang, J.-H., Chung, T. D. Y., and Oldenburg, K. R. (1999) A simple statistical parameter for use in evaluation and validation of high throughput screening assays. *J. Biomol. Screening* 4, 67–73.
- (90) Quirós, L. M., Aguirrezabalaga, I., Olano, C., Méndez, C., and Salas, J. A. (1998) Two glycosyltransferases and a glycosidase are involved in oleandomycin modification during its biosynthesis by *Streptomyces antibioticus*. *Mol. Microbiol.* 28, 1177–1185.
- (91) Williams, G. J., Zhang, C., and Thorson, J. S. (2007) Expanding the promiscuity of a natural-product glycosyltransferase by directed evolution. *Nat. Chem. Biol.* 3, 657–662.
- (92) Fernández-Irigoyen, J., Santamaría, E., Chien, Y., Hwu, W., Korman, S. H., Faghfoury, H., Schulze, A., Hoganson, G. E., Stabler, S. P., Allen, R. H., Wagner, C., Mudd, S. H., and Corrales, F. J. (2010) Enzymatic activity of methionine adenosyltransferase variants identified in patients with persistent hypermethioninemia. *Mol. Genet. Metab.* 101, 172–177.
- (93) Panmanee, J., Bradley-Clarke, J., Mato, J. M., O'Neill, P. M., Antonyuk, S. V., and Hasnain, S. S. (2019) Control and regulation of S-adenosylmethionine biosynthesis by the regulatory β subunit and quinolone-based compounds. *FEBS J.* 286, 2135–2154.
- (94) Murray, B., Antonyuk, S. V., Marina, A., Lu, S. C., Mato, J. M., Hasnain, S. S., and Rojas, A. L. (2016) Crystallography captures catalytic steps in human methionine adenosyltransferase enzymes. *Proc. Natl. Acad. Sci. U. S. A. 113*, 2104–2109.
- (95) Schubert, H. L., Blumenthal, R. M., and Cheng, X. (2003) Many paths to methyltransfer: A chronicle of convergence. *Trends Biochem. Sci.* 28, 329–335.
- (96) Cheng, X., and Blumenthal, R. M. (2008) Mammalian DNA methyltransferases: A structural perspective. *Structure* 16, 341–350.
- (97) Sánchez-Pérez, G. F., Bautista, J. M., and Pajares, M. A. (2004) Methionine adenosyltransferase as a useful molecular systematics tool revealed by phylogenetic and structural analyses. *J. Mol. Biol.* 335, 693–706.
- (98) Lukinavičius, G., Lapinaitė, A., Urbanavičiūtė, G., Gerasimaitė, R., and Klimašauskas, S. (2012) Engineering the DNA cytosine-5 methyltransferase reaction for sequence-specific labeling of DNA. *Nucleic Acids Res.* 40, 11594–11602.
- (99) Huber, T. D., Johnson, B. R., Zhang, J., and Thorson, J. S. (2016) AdoMet analog synthesis and utilization: current state of the art. *Curr. Opin. Biotechnol.* 42, 189–197.
- (100) Tomkuvienė, M., Mickutė, M., Vilkaitis, G., and Klimašauskas, S. (2019) Repurposing enzymatic transferase reactions for targeted labeling and analysis of DNA and RNA. *Curr. Opin. Biotechnol.* 55, 114–123.

(101) Deen, J., Vranken, C., Leen, V., Neely, R. K., Janssen, K. P. F., and Hofkens, J. (2017) Methyltransferase-directed labeling of biomolecules and its applications. *Angew. Chem., Int. Ed.* 56, 5182–5200